Original Article

JCBFM

Journal of Cerebral Blood Flow & Metabolism
2019, Vol. 39(5) 782–793

DOI: 10.1177/0271678X17751835
journals.sagepub.com/home/jcbfm


Hybrid PET/MRI imaging in healthy unsedated newborn infants with quantitative rCBF measurements using ^{15}O-water PET

Julie B Andersen[1], Ulrich Lindberg[1], Oline V Olesen[1,2], Didier Benoit[1], Claes N Ladefoged[1], Henrik BW Larsson[1], Liselotte Højgaard[1], Gorm Greisen[3] and Ian Law[1]

Abstract

In this study, a new hybrid PET/MRI method for quantitative regional cerebral blood flow (rCBF) measurements in healthy newborn infants was assessed and the low values of rCBF in white matter previously obtained by arterial spin labeling (ASL) were tested. Four healthy full-term newborn subjects were scanned in a PET/MRI scanner during natural sleep after median intravenous injection of 14 MBq ^{15}O-water. Regional CBF was quantified using a one-tissue-compartment model employing an image-derived input function (IDIF) from the left ventricle. PET rCBF showed the highest values in the thalami, mesencephalon and brain stem and the lowest in cortex and unmyelinated white matter. The average global CBF was 17.8 ml/100 g/min. The average frontal and occipital unmyelinated white matter CBF was 10.3 ml/100 g/min and average thalamic CBF 31.3 ml/100 g/min. The average white matter/thalamic ratio CBF was 0.36, significantly higher than previous ASL data. The rCBF ASL measurements were all unsuccessful primarily owing to subject movement. In this study, we demonstrated for the first time, a minimally invasive PET/MRI method using low activity ^{15}O-water PET for quantitative rCBF assessment in unsedated healthy newborn infants and found a white/grey matter CBF ratio similar to that of the adult human brain.

Keywords

Cerebral blood flow, neonatology, PET/MR, positron emission tomography, arterial spin labeling

Received 29 June 2017; Revised 3 December 2017; Accepted 4 December 2017

Introduction

The clinical importance of white matter injury or periventricular leukomalacia (PVL) in the premature infant has been recognized in neonatal neurology for more than four decades,[1] as a leading cause of long-term motor and cognitive disability. The etiological understanding has centered on hypoxic-ischemic and infectious/inflammatory damage, but nutritional and hormonal factors may also contribute.[2] Given that the white matter is a vascular end-zone and a predominant area for injury in the neonatal patient, knowledge of the exact quantitative regional cerebral blood flow (rCBF) value in the healthy newborn can contribute in understanding the underlying pathophysiology of PVL in preterm infants.

Measuring rCBF in newborn infants presents substantial technical and ethical concerns. Regional CBF in newborn infants is known to be relatively low in

[1]Department of Clinical Physiology, Nuclear Medicine and PET, Rigshospitalet, University of Copenhagen, Copenhagen, Denmark
[2]DTU-Compute, Technical University of Denmark, Kongens Lyngby, Denmark
[3]Department of Neonatology, Rigshospitalet, University of Copenhagen, Copenhagen, Denmark

Corresponding author:
Julie B Andersen, Department of Clinical Physiology, Nuclear Medicine and PET, Rigshospitalet, University of Copenhagen, Blegdamsvej 9, Copenhagen 2100, Denmark.
Email: juliebjerglund@gmail.com

white matter,[3,4] challenging the accuracy of the applied methods. In addition, the brains of newborn infants are both smaller and vary in anatomical structure and tissue maturity including the developmental stage of myelination when compared to the adult brain.[5,6] Quantitative ^{15}O-water PET is considered the 'gold standard' for rCBF measurements in humans[7,8] but existing PET rCBF studies in the neonatal population are few, and were performed decades ago with a generation of lower resolution PET scanners and on infants with neuropathology or suspected neuropathology.[9–11] Present day state-of-the-art PET imaging methods have improved significantly and may more appropriately address the technical issues found in these pioneering studies. Furthermore, there are no studies in healthy newborns to address what true normal rCBF values are in this age group.

Although there is a far more accessible and non-ionizing alternative imaging technique for rCBF measurements than PET in the form of arterial spin labeling (ASL) using MRI, only a limited number of neonatal publications are available.[12–19] Methodological challenges for ASL, such as variability of arterial transit time and obtaining a sufficient signal-to-noise ratio, are especially challenging in the neonatal population with small organs and generally low rCBF[20] and may significantly affect both rCBF distribution and quantitative values.

The purposes of this study was to apply a newly developed method in healthy newborn subjects using PET with ^{15}O-water and an image-derived input function (IDIF) from the left ventricle previously developed in a piglet model on a hybrid PET/MRI scanner.[21] This method utilizes the extended axial field of view of the scanner (25.8 cm) to acquire dynamic data from both brain and heart simultaneously and obtains quantitative minimally invasive measures of rCBF with a radioactive dose sufficiently low to be acceptable for medical research in this subject group. PET/MRI allows simultaneous co-registered CBF measurements with ^{15}O-water PET and ASL(PASL) MRI allowing the best possible scenario to estimate accuracy of CBF values from ASL. This strategy has been used previously in adults,[22] but never in the neonatal group. We aimed to investigate if the surprisingly low values of white matter rCBF (~3 ml/100 g/min) that have been reported in healthy newborn control subjects using single TI PASL MRI[16,19] could be reproduced using ^{15}O-water PET. By doing this, we aimed to establish a proof-of-concept of the new PET/MRI method in newborn infants. This could be a useful method for future imaging investigations of preterm infants, including better understanding of the underlying pathophysiology and significance of changes in rCBF in neonatal PVL.

Material and methods

Subjects

Four healthy newborn infants participated in the rCBF measurements with ^{15}O-water PET and PASL MRI scans on a hybrid PET/MRI scanner (mMR, Siemens, Erlangen, Germany). All had an uncomplicated postnatal period. See Table 1 for details of individual characteristics.

The newborn infants were recruited one to two days after birth while hospitalized in the obstetric ward. Eighty parents were asked to participate and four families agreed to participate. The main reasons declining participation by the majority of parents were: (1) practical issues regarding time and place, (2) possible adverse effects of radiation exposure to the child and (3) reduced mental resources to cope with the procedure and scan.

Ethical considerations

According to EU legislation, effective dose limits for members of the general public have been set to 1 mSv/year in addition to the average annual background exposure to ionizing radiation 2.4 mSv/year.

Table 1. Subject characteristics.

Subject	Gender	Age (d)	Para	GA (w+d)	Birth Weight (g)	Delivery	Apgar	pH (A/V)	$H_2{}^{15}O$ (MBq)
1	M	2	1	40 + 1	3262	Vaginal	10, 10, 10	7.21/7.35	14
2[a]	M	3	3	40 + 1	3664	Vaginal	10, 10, 10	7.33/7.39	15
3	M	3	2	38 + 4	3438	C-section	8, 9, 10[b]	7.13/7.34	14
4[c]	M	2	1	38 + 2	3246	C-section	10, 10, 10	7.32/7.38	14

[a]Mother with Lub-antibodies with titer 1. Infant with maximum serum-bilirubin level 127. No intervention. [b] Color and tone. [c]Child with infrequent eye contact and delayed eyesight development. Normal eye exam and normal structural external anatomy. Normal development on 1 year clinical follow-up. GA: gestational age. Note: Para (*para gravida*): the number of pregnancies. Apgar: the Apgar score of newborn infants at 1, 5, 10 min after birth. pH (A/V): Postpartum umbilical cord arterial and venous pH.

One mSv/year is also the effective dose limit for special protection of the unborn child in pregnant workers, e.g. medical staff, during the pregnancy,[23] and the upper dose limit recommendation set by the International Commission on Radiological Protection (ICRP) for 'individuals that are exposed from a single dominant source that gives them little or no individual benefit but benefits to society in general'. This dose corresponds to the radiation thresholds defined in the European Commission guidance on medical exposure for biomedical research,[24] which states that up to 0.1 mSv may be used for research aiming at 'increasing knowledge', while up to 1 mSv may be used for research aiming at 'health benefits'. The probability of a fatal radiation induced cancer has been estimated to approximately 0.005% per mSv effective dose for the whole population with its normal age distribution. For children up to the age of 10 years, the probability of fatal cancer induction is assumed to be two to three times higher for safety reasons.[23,25] Thus, we set an upper effective dose limit in this study of 0.33 mSv, which incidentally is comparable to the background radiation dose per month for the general public in Denmark (4.0 mSv/year). This dose corresponds to an injected activity of 14–15 MBq ^{15}O-water per injection or approximately 4.3 MBq/kg to infants with a mean weight of 3.4 kg. The activity administered to each child was calculated based on an approximate weight at scanning which was assumed to be 10% lower than the birth weight (Table 1).

The study was approved by the Regional Scientific Ethical Committee of the Capital Region of Denmark, protocol no. H-6-2014-081 and oral and written informed consent was obtained from the children's parents prior to the examination according to the Helsinki II declaration.

PET and MRI acquisition

An experienced pediatrician placed a small polyethylene catheter (24 G) in a vein in the hand or cubital vein. The child was given a sugary solution orally for pain relief during the procedure. In the scanner, the infants were swaddled and slept naturally after feeding. They were monitored with arterial saturation and electro cardiogram, displayed on a monitor placed in the control room. Hearing protection ('mini-muffs') was placed over the ears. The head was immobilized by small pillows on both sides. In the last three subjects, a real-time surveillance system, TCL2,[26] with a 3D-camera for monitoring and tracking motion of the head and face was applied throughout the scan, enabling the parents and staff to view the child's movements and evaluate depth of sleep indirectly. The system is an MRI functional version of TCL1[27,28] (see Figure 1 and supplementary materials for a short video clip of the monitoring feedback).

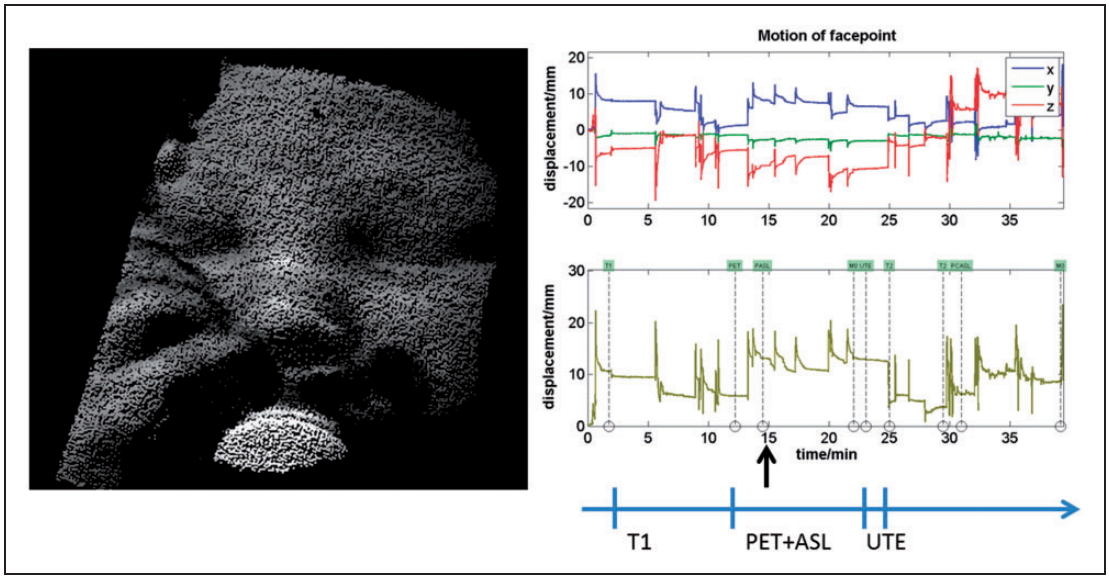

Figure 1. MRI compatible motion tracking system of subject no. 2. A real-time motion tracker and surveillance system applied for infants in the PET/MRI scanner with 3D surface images of the face and right hand of the infant (left) and tracking of movements on a plot (right) with displacement in mm in three directions (right top) and the resulting summed displacement in mm (right bottom). The arrow points to time of tracer injection. There are rapid head movements with displacements of 5 mm during scanning returning to baseline. This circumstance will not significantly affect rCBF PET measurements, but are detrimental for ASL images.

For the child without video-monitoring, heart rate was used as a measure of alertness. Infant no. 3 woke up 70 s after the tracer had been injected and no ASL data were obtained.

The infants were imaged using a 16-channel mMR head-neck array coil. High resolution 3D T1-weighted imaging (T1w MP-RAGE) was performed for anatomical imaging with the following parameters: Matrix size = 256 × 256, slice thickness = 1 mm, echo time (TE) = 2.44 ms, TR = 1900 ms, FOV = 250 mm, flip angle 9°. In one of four children, 2D T2-weighted images (BLADE) were acquired subsequently with the following parameters: Matrix size: 320 × 320, slice thickness = 5 mm, TE = 118 ms, TR = 6000 ms, flip angle 125°.

In two of three infants, ASL data acquisition was performed simultaneously with the PET scan. For the last infant, the ASL scan was performed immediately after the PET scan. The change of procedure was done to avoid audible noise from the MRI during the PET scanning, which was observed to cause stirring of the first two infants. Pulsed ASL scans lasted 7 min and planning of the sequence was done on the T1w MP-RAGE. ASL was performed with the standard Siemens protocol (PICORE-Q2TIPS) (See supplementary material for imaging parameters of ASL).

Dynamic PET scans were started approximately 60 s before 14 or 15 MBq ^{15}O-water was injected IV by hand as a short bolus (1–2 ml) through an additional tubing of approximately 75 cm filled with isotonic saline with a volume of 1 ml. The catheter was immediately flushed with 2 ml isotonic saline. Data were collected in list-mode for 8 min. On T1w MP-RAGE, it was verified that both brain and heart were in the axial field of view in all subjects.

MRI-based attenuation maps for PET attenuation correction (AC) of the brain region were derived using the vendor provided ultrashort echo time (UTE) imaging with repetition time/TE 1/TE 2 = 11.94/0.07/2.46 ms, flip angle 10°, reconstructed on 192 × 192 × 192 matrices (1.6 × 1.6 × 1.6 mm^3). The PET attenuation maps were created in the following manner: AC was based on an in-house method called RESOLUTE, a fully automatic method that segments air, brain, and soft tissue voxels on the UTE images, and uses a mapping of R_2^* values to Hounsfield units to obtain patient specific continuous bone density value.[29] The bone extraction was limited to the head to minimize noise. Similarly, the lungs were based on a semi-automatic segmentation method using the R_2^* signal.

PET data analysis

The PET images were reconstructed using maximum likelihood estimation method (MLEM) performing 42 iterations with one subset and a voxelsize of 2.1 × 2.1 × 2.0 mm^3. The data were sorted in the following manner in subject no. 1 and 2: 1 × 60 s, 15 × 2 s, 11 × 5 s, 12 × 10 s, 4 × 20 s, 1 × 135 s, subject no 3: 1 × 60 s, 35 × 2 s, subject no 4: 1 × 40 s, 15 × 2 s, 11 × 5 s, 12 × 10 s, 4 × 20 s, 1 × 155 s. The length of the first frame accounts for the delay between scanner start and injection time (Figure 2) necessary for sequence initiation. Images were reconstructed with a Gaussian reconstruction filter of 2 mm and corrected for randoms, dead time and decay. Note that for display purposes, the PET images are shown after a 5 mm Gaussian filtering (Figures 4 and 5).

All PET analysis was done in PMOD (Zürich, Switzerland). A whole brain region was manually drawn as a VOI along with a total of 11 regional VOIs on the T1w MP-RAGE image: frontal and occipital periventricular unmyelinated white matter, frontal cortex, occipital cortex, perirolandic cortex, thalamus, striatum, mesencephalon, pons and medulla and central myelinated white matter in the corticospinal tracts above the insula identified by a higher signal intensity on the T1-weighted images indicating increased lipid content (Figure 3). The cortical VOIs followed the structure boundaries closely. Periventricular white matter VOIs were drawn approximating on the primarily lesion sites for PVL with a minimum of 4 mm distance to grey matter to avoid activity spill-in. Measurements were obtained in the right and left side of the cerebrum. A 1-tissue compartment model adapted to ^{15}O-water PET studies was applied. K_1(rCBF), k_2 and delay were fitted simultaneously as proposed in Meyer.[30] The dispersion was not fitted but was set to 0 s. The equation is as shown in our previous report.[21] The length of the fit was 180 s from injection time.

The extended axial field-of-view of 25.8 cm of the scanner allowed for simultaneous coverage of the whole brain and heart (see Figure 1 in supplementary material). The IDIF was generated from the dynamic PET sequence as described in our previous report.[21] A box-shaped VOI containing the left ventricle of the heart was defined on the T1w MP-RAGE and projected to the summed PET image of the first 16 s after bolus injection filtered by a 3D Gaussian 6 mm filter. Within this VOI, the 30 voxels (0.26 ml) with highest activity was selected and used to extract the IDIF from the dynamic PET sequence. On the T1w MP-RAGE, the positioning of the IDIF VOI was evaluated, with the placement in the center of the left ventricle at a distance of a minimum 5 mm from the myocardial wall. The apical length of the left ventricle was average 2.8 cm (range 2.6–3.0 cm) and the diameter of the left ventricle was average 1.4 cm (range 1.3–1.6) based on three of the four subjects' T1w MP-RAGE images.

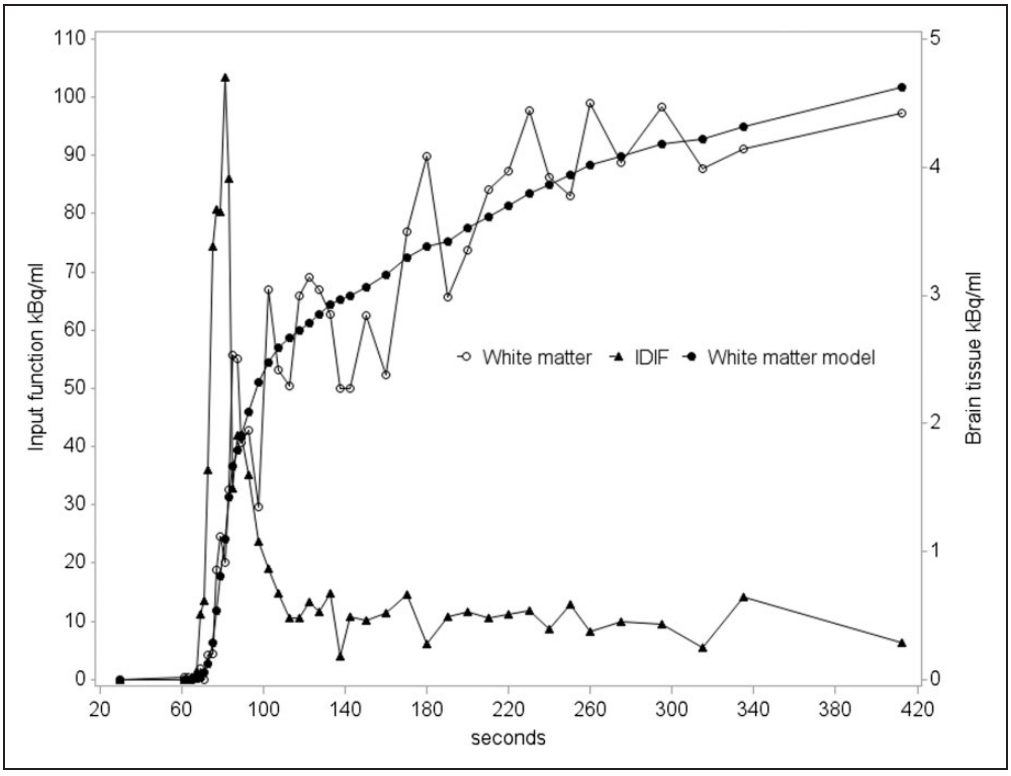

Figure 2. Blood and tissue time activity curves. The IDIF time activity curve extracted from a volume of interest in the left ventricle of the heart (triangles) from subject no. 1. The original IDIF curve is shown without correcting for delay. Tissue activity curve from frontal and occipital periventricular unmyelinated white matter (circles) and the model fit curve (dots). The tissue activity and IDIF are shown using different scales.

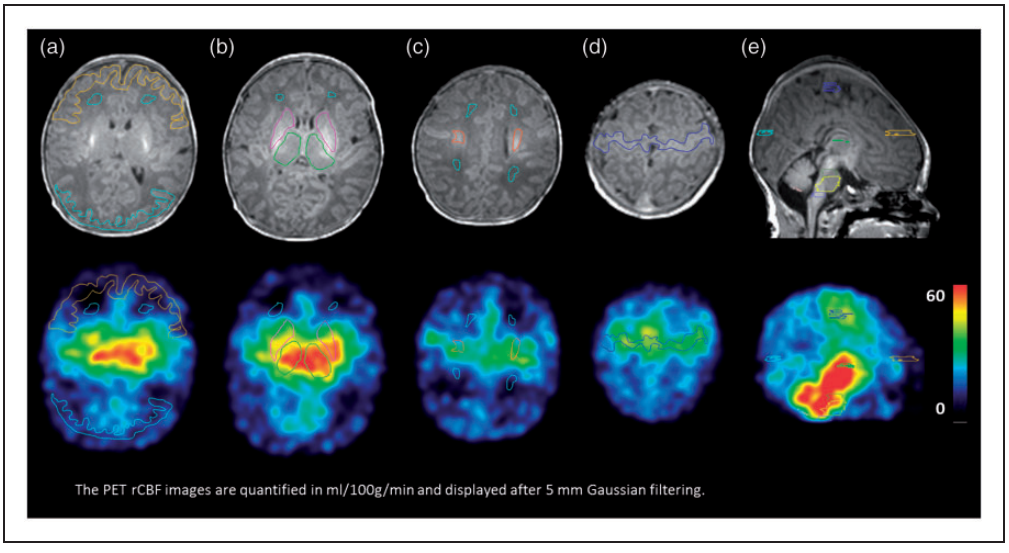

Figure 3. Axial (a-d) and sagittal (e) images of subject no. 1 documenting volumes-of-interest (VOIs). T1w MP-RAGE MRI is shown at the top at the level of the basal ganglia (a+b), the centrum semiovale (c), perirolandic cortex (d) and the corpus callosum (e). In (a) frontal and occipital cortex (yellow and blue) and frontal periventricular unmyelinated white matter (dark green) is displayed. In (b) thalami (green) and striatum (pink) and frontal unmyelinated white matter (dark green) is shown. In (c) frontal and occipital unmyelinated white matter (dark green) and myelinated white matter in the centrum semiovale (orange) is shown. In (d) the perirolandic cortex (blue) is shown. In (e) the cortex from occipital (light blue), frontal (yellow) and perirolandic (blue) is shown. The PET rCBF images are quantified in ml/100 g/min and displayed after 5 mm Gaussian filtering.

Because of movement artefacts, the left ventricle of the last subject could not be measured precisely.

Statistical analysis

Regional CBF values from PET are presented as mean rCBF values, 95% confidence intervals (CI) and coefficient of variation (COV) from the four subjects.

Results

Dynamic PET data were obtained in all four subjects without sedation. Three subjects had 7-min acquisitions and one had a 70 s acquisition after tracer injection with early termination due to movements. The fitted delay in the four subjects ranged from −0.97 s to 0.38 s with a mean value of −0.32 s. These values reflect the short distance from the left ventricle to the brain (approximately 10–15 cm in a term infant) and an accordingly short time-shift of the tracer from heart to brain (less than a second). As expected, the fitted delay values vary within a single frame length (2 s).

All subjects had developmentally normal brain T1w MP-RAGE images. This includes normal cortical folding and the expected distribution of increased signal intensity in the myelinated white matter of the posterior third of the internal capsules, thalami, mesencephalon and the central portion of the centrum semiovale.

For anatomical correlation to PET imaging of the heart, T1w MP-RAGE imaging covered the thorax. The input curve for the IDIF was obtained from the left ventricle from all subjects. A plot of the original IDIF and whole brain tissue curves of subject no. 1 are shown in Figure 2.

The rCBF PET distribution is shown in Figures 4 and 5, which shows PET with relatively high rCBF in the striatum, thalami, mesencephalon, pons, cerebellar vermis, and medulla, and to a lesser degree in the perirolandic cortex, mesial occipital cortex and hippocampal area.

The average quantified rCBF PET measurements for periventricular unmyelinated white matter were 10.3 ml/100 g/min (range: 9.3–11.5 ml/100 g/min). The whole brain PET CBF values are shown in Table 2. The average ratio between thalamic rCBF and unmyelinated white matter was 0.36 (range: 0.24–0.40). The left hemisphere had a significantly higher mean CBF 10.1 ml/100 g/min than the right hemisphere 9.0 ml/100 g/min ($p = 0.01$).

The calculations of rCBF ASL in subjects 1 and 2 show areas of high focal CBF related to the position of known arteries in the insula and the mesial and lateral

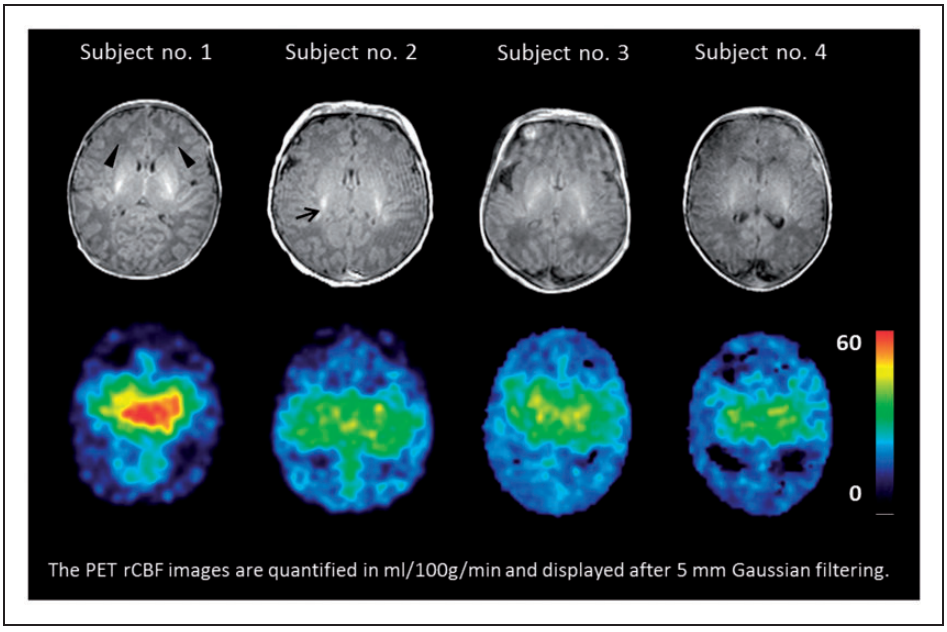

Figure 4. Axial rCBF images of four newborn infants (1–4) using PET/MRI. Axial T1w MP-RAGE MRI is shown at the top at the level of the basal ganglia. The myelination of the white matter is seen in the posterior internal capsule as increased signal intensity (arrow). The white matter frontally and occipitally has a low signal intensity (arrowheads) indicating low degree of myelination as expected in imaging of infants at term.[45] Infant no 3 only had 70 s PET acquisition. The PET rCBF images are shown after 5 mm Gaussian filtering and quantified in ml/100 g/min. Particularly, high rCBF is found in the striatum and thalami and low rCBF is seen in lateral frontal and occipital white matter and cortices.

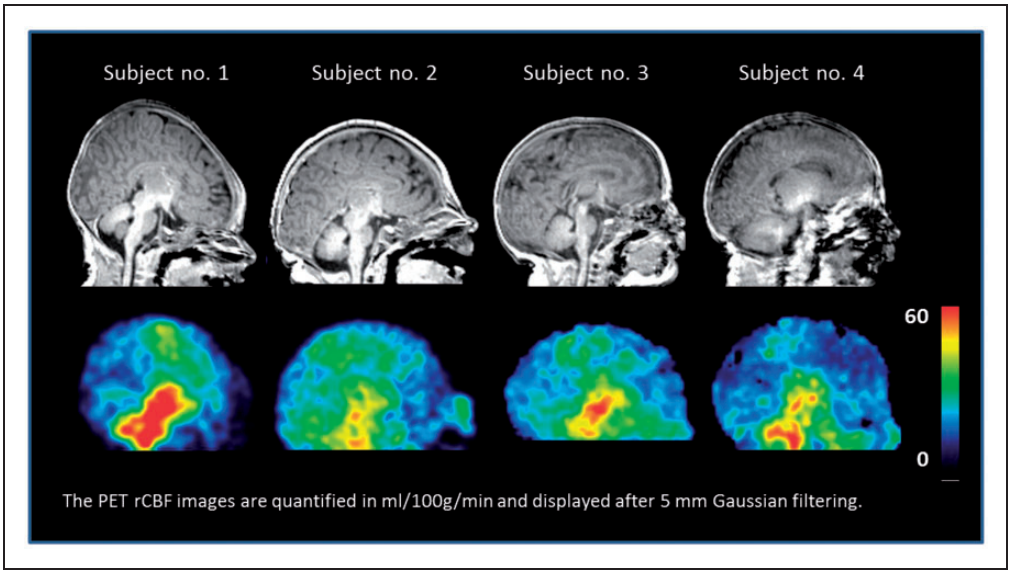

Figure 5. Sagittal rCBF images of four newborn infants (1–4) using PET/MRI. Sagittal T1w MP-RAGE MRI is shown at the top at the level of the corpus callosum. The PET rCBF images are shown after 5 mm Gaussian filtering and quantified in ml/100 g/min. Relatively, high rCBF is seen on the PET images in the thalami, mesencephalon, pons, cerebellar vermis, and medulla, and to a lesser degree in the perirolandic cortex.

cortices. In subject 4, there is relatively high cortical rCBF in the frontal lobes with a defect in the occipital areas (see supplementary material). In all three subjects, the distribution of the rCBF ASL values deviated significantly from both the simultaneous PET rCBF measurements, and the expected rCBF found in previous ASL studies[16,20] and were, therefore, interpreted as too technically inadequate and unreliable to analyze further.

No ASL data were obtained in subject 3 because the infant woke up before scanning.

Discussion

This study is a human implementation of an experimental set-up for simultaneous rCBF measurements using ^{15}O-water PET and ASL on a hybrid PET/MRI scanner that we have previously employed in piglets.[21] In that study, we documented that reliable whole brain CBF values could be obtained even at a very low injected activity of 20 MBq ^{15}O-water using an IDIF from the heart. We found that whole brain CBF ASL and CBF PET were congruent during baseline but not during hyperperfusion. The results were, however, encouraging enough to translate to human studies. In newborn infants, we expected better quality data because of larger brain size (brain weight in piglets 3 weeks old 50 g and in newborn infants approximately 350–400 g), particularly in the estimation of white matter rCBF that could not be segmented reliably in piglets because of resolution limitations. Furthermore, the input function derived from the heart should be valid since the VOI in the heart is of similar size: the left ventricular long-axis is approximately 2.6 cm in three week old piglets[31] and was measured to be 2.8 cm in three of the four newborn infants in this study. An important difference between the present study and the animal studies was the lack of sedation in the infants. This circumstance increases the risk of image degradation due to head movements, but allows measurement of the native rCBF distribution uninfluenced by sedatives. Avoiding sedation was safest, but also a condition for the inclusion of healthy volunteers. A very low injected activity of 14–15 MBq ^{15}O-water allowed imaging of sufficient quality at a radiation dose low enough to be acceptable for medical research. Besides corroborating existing estimates of global CBF in healthy term infants obtained by a range of methods, each having their own assumptions, we present the first normal rCBF values in this population. As the presented method relies on an IDIF,[21] the new method cannot be referred to as 'gold standard'. However, since PET is based on relative few assumptions, and since we have explored the sources of error and their magnitude in a newborn piglet model (e.g. the possible overestimation due to the noninvasive determination of the input function), we consider the results reliable. The use of an IDIF would not affect the rCBF distribution that is better defined by ^{15}O-water PET than with ASL MRI due to the longer half-life of ^{15}O-water. The method is an adaptation of classical rCBF PET

methodology using state-of-the-art hardware, and can serve as a valuable tool for the comparison, evaluation and optimization of more clinically available methods, such as ASL MRI in the neonatal population.

Even though we had a low participation rate of families, we don't believe this affected the result's representativeness, but rather highlighted the difficulties in recruiting infants to research projects that do not directly benefit the parents nor infant.

Since PET inherently involves ionizing radiation, a pediatric PET research method should be reliable, quantitative, and ethically and clinically acceptable in terms of minimal invasiveness and radiation dose, by complying with the principles of ALARA ("as low as reasonably achievable").[32] The level of what is applied in our study is well within what EU legislation for radiation dose in healthy children. This tracer dose (0.33 mSv per injection in this study) could also be applied in scientific protocols in a patient group of infants with prematurity or neuropathology such as PVL, aiming directly at the diagnosis, cure, or prevention of disease.[24,25] It should be noted that most data regarding the absorbed dose estimates of ^{15}O-water in pediatric patients from ICRP80 are based on adult data.[33] ^{15}O-water kinetics is simple, and because of the short half-life of the isotope (122 sec), the radiation dose is limited. However, when following the present precautionary principle model, one should always carefully consider the clinical value of a study using ionizing radiation in pediatric patients.

In the present study, the left ventricle of the heart could comfortably be contained in the extended axial FOV of the scanner enabling dynamic sampling of the IDIF in a large blood volume. The IDIF alleviated the need for invasive arterial blood sampling while still enabling a valid quantification of rCBF. The IDIF method for quantitative PET measurements has been thoroughly investigated in the literature using different approaches to optimize the input curve.[34–36] In newborn infants, only one previous study applied the left ventricle for IDIF extraction and quantitative glucose uptake values.[37] In our study on piglets, we observed an overestimation of approximately 20% when compared to gold standard arterial blood sampling which may in part be explained by the 3-s time framing used as opposed to 1- and 2-s framing giving a better time resolution and minimizing the underestimation of the peak of the input curve. We applied 2-s time framing in the PET data reconstruction of the newborn infants to minimize this effect. However, since the structures in question are small (the left ventricle of the heart is approximately 2 mL in a full term neonate[38] and the applied VOI in the left ventricle was 0.26 mL), partial volume effects and resolution recovery may influence the values obtained from the dynamic time framing leading to an underestimation of the values in the IDIF. Consequently, there is a possible overestimation of rCBF values in this first human study, but considering that the values in question are relatively small especially in white matter, the implications for the conclusions of this study are modest. With present ASL MRI techniques, quantified rCBF in white matter is neither reliable in adults nor neonates owing to the prolonged arrival time of magnetized blood to the periventricular watershed areas.[39,40] However, use of multi-delay (TI) ASL approach to quantify both arrival time and CBF can improve quality of the ASL data,[41,42] presumably also in the neonatal patient group.

The normal metabolic development of the brain of newborn patients with suspected pathology has been investigated in a limited number of FDG PET studies.[6,43,44] The studies showed increased activity in the sensorimotor area, basal ganglia and the brainstem. At birth, myelination of white matter has reached the cortical tracts passing through the centrum semiovale in the internal capsule and cortical spinal tracts relating to the sensorimotor cortex. Hence, the myelin is visible on MRI imaging.[5,45] In our PET/MRI study on healthy subjects, this known myelination pattern was replicated as high signal intensity changes on T1w MP RAGE images. Noticeably, increased rCBF could be seen in the corresponding areas on the PET image (Figure 4) and in the quantified rCBF values (Table 2), which correlates to the myelination process in cortical and subcortical areas. This result can be interpreted as an expression of the known neuro-vascular coupling between metabolism and tissue perfusion. In line with these findings, the frontal and occipital periventricular unmyelinated white matter, showing low intensity signal on T1w MPRAGE images, had substantially lower PET rCBF values (Table 2) with a mean of 10.3 ml/100 g/min. This result correlated to the myelination process in these areas occurring much later between one and two years of age.[5]

Previous ^{15}O-water PET studies performed in infants with neuropathology[9–11] were performed in 2D acquisition mode with low spatial PET scanner resolution of 11.7 and 18 mm and gave an effective radiation dose of 5.8 mSv for each injection. Reliable quantification of rCBF was challenged by the collection of only a few arterial blood samples to estimate the input function, which was not corrected for delay nor dispersion. An alternative method to avoid direct arterial sampling in older children has been to use a standard arterial input function to calculate the rCBF distribution that is scaled by quantitative global CBF calculated from the clearance of ^{15}O-water, k_2.[46,47] However, our subject group requires hand held injection for safety reasons to provide the required control over injected activity and volume, and the arterial input function shape,

Table 2. Quantified regional CBF results.

rCBF (ml/100 g/min)	Subject 1	Subject 2	Subject 3	Subject 4	Mean (95% CI)	COV (%)
White matter unmyelinated	10.1	11.5	10.1	9.3	10.3 (8.8;11.7)	8.9
White matter myelinated	23.3	15.9	14.6	10.6	16.1 (7.6;24.5)	32.9
Frontal cortex	15.7	12.9	9.3	10.7	12.2 (7.7;16.6)	23.0
Occipital cortex	18.4	16.3	13.2	12.3	15.1 (10.6;19.5)	18.7
Striatum	55.9	24.9	34.1	33.3	37.1 (16.0;58.1)	35.7
Thalamus	42.9	30.3	29.3	22.5	31.3 (17.7;44.8)	27.2
Mesencephalon	52.8	37.8	43.3	47.7	45.4 (35.2;55.6)	14.1
Pons	48.5	35.0	38.4	43.6	41.4 (32.0;50.8)	14.3
Medulla	57.2	38.8	47.7	53.9	49.4 (36.5;62.3)	16.4
Perirolandic cortex	33.2	18.4	13.9	14.2	19.7 (6.0;33.4)	43.7
Right hemisphere	12.4	7.2	8.7	7.5	9.0 (5.1;12.8)	26.7
Left hemisphere	13.4	8.2	9.6	9.3	10.1 (6.5;13.7)	22.4
Whole brain	22.2	17.8	16.2	15.0	17.8 (13;23)	17.7
Ratio white matter/thalami	0.24	0.38	0.40	0.41	0.36 (0.23;0.48)	22.2

Note: Regional CBF, mean, 95% confidence intervals (CI) and coefficient of variation in percent (COV) of four newborn infants scanned on the hybrid PET/MRI system with ^{15}O-water PET. Values in mL/100 g/min. Ratio is the ratio between rCBF of unmyelinated white matter and thalami. In subject no 3, the PET values were fitted over 70 s, where the other three PET scans were fitted over 180 s. COV: coefficient of variation; rCBF: regional cerebral blood flow.

delay and dispersion in infants have not yet been adequately described. These assumptions may be avoided using an IDIF method based on actual measurements. As the proposed method is dependent on the inclusion of both brain and heart in the extended axial field of view of the PET/MRI scanner, this option will only be feasible until the age of nine months to one year, depending on the height of the child and with the field of view of the current clinically available PET/MRI scanner.

None of the aforementioned PET imaging studies[9–11] could give reliable estimates of white matter rCBF, because of the poor resolution of the scanners, but all have indicated that the white matter rCBF is very low in newborn infants and that the ratio to basal ganglia CBF may be as low as 0.23 when measured with SPECT.[3] We found a mean CBF ratio of white matter to the thalami of 0.36 which is in the range of values measured in the adult brain (0.30–0.48).[48–51] Regional CBF values from previous studies on term infants with varying degree of neuropathology, ranged from 9 to 76 ml/100 g/min.[9,10,52] The large variation may be caused by the above-mentioned methodological inadequacies, the effects of pathology, and the developmental span.[53] Global CBF in premature infants measured with ^{133}Xenon was 20 ml/100 g/ml in non-distressed infants.[54]

Regional CBF in white matter has not been reported previously with modern PET methods in healthy newborn infants. Regional CBF using ASL MRI in periventricular unmyelinated white matter in healthy infants[12,16] has been measured to be between 2.3 and 3.6 mL/100 ml/min or 1/10 of basal ganglia rCBF, which is outside the 95% CIs found in this PET study of 10.3 mL/100 ml/min (95% CI 8.8;11.7 mL/100 ml/min) and 1/3 of thalami rCBF (ratio, 0.36, 95% CI 0.23;0.48). The ASL rCBF values are critically dependent on arrival time of magnetically labeled inflowing arterial blood to the tissue, and delayed arrival can be the cause of falsely reduce rCBF.[55,56] Unfortunately, our own ASL data could not be used to further illuminate the matter. At the time of our studies, the ASL MRI sequence available to us was a single TI pulsed ASL (pASL) sequence. Our assumption was that we could obtain better ASL image quality and data in the larger brains of the infants than in the piglet study by our group.[21] Motion artefacts are however a problem for ASL in this age group: 25% of scans were discarded because of poor image quality in the study by Boudes et al.[20] and 40% in the study by Miranda et al.[15] Unfortunately, the ASL scans of all our subjects were substantially affected by motion artefacts as documented with the on-line marker-less tracking system (Figure 1) and must be considered unreliable. In a clinical setting where sedation is permissible for diagnostic imaging, motion artefacts could be less significant. It would, however, be preferable to avoid sedation and correct for movement.[27] For subject no. 1 and 2, there was a pronounced vascular signal that could be attributed to insufficiencies in sequence parameters or the sequence itself. Comparative studies in newborns have recommended pseudo-continuous arterial spin labeling (pCASL) as the superior technique that

allowed improved image quality with a more detailed identification of the different brain structures[20] in accordance with the ASL white paper recommendations.[57] Furthermore, as mentioned previously multidelay (TI), ASL could improve quality of the data[41,42] especially in low CBF areas (see supplementary material for ASL rCBF images of the subjects).

Interruption of the supply of nutrients and oxygenation can cause PVL in vulnerable areas of the periventricular white matter. Assessing changes in perfusion in white matter is of value in the clinical work-up of PVL patients and cannot be easily assessed with clinically available methods (near infrared spectroscopy (NIRS) and Doppler ultrasound). For this reason, the implementation of a PET imaging technique with high spatial resolution could possibly be of importance in evaluating the severity of PVL. As a one-stop scan, PET alongside advanced MRI in a PET/MRI could potentially add to the value of imaging for predicting severe neurodevelopmental deficits such as debilitating cerebral palsy.[58] Logistics and safety issues when considering PET/MR scans of premature infants can be addressed by performing the scan using an MR-compatible infant transport incubator which is available for the PET/MR scanner.

PET image quality and resolution in a premature infant of, i.e. 30 weeks' gestational age should be adequate since the unmyelinated white matter is the most prominent tissue class of the brain and the gyral pattern is relatively simple.[59] The anatomical structures are sufficiently developed to enable adequate VOIs to determine white and gray matter rCBF, even though the brain volume is small and increases dramatically from 150 mL at 29 weeks to 400 ml at term.[59] The volume of the left ventricle in premature infant of 1 kg is approximately 1 mL corresponding to a diameter of 14 mm if assuming a spherical shape,[38] which would still allow the measurement of central voxels that are not affected by the partial volume effect.

Even though we were unsuccessful in acquiring adequate ASL data, we believe that we have presented a clinical neuropediatric tool for future PET/MRI in the healthy or diseased child during the first year of infancy. In neonatal patients, particularly, PVL is a target diagnosis, where current diagnostic methods are challenged to adequately quantify CBF and characterize the extent of the white matter damage and relate it to anatomy. This should now be possible.

Furthermore, it would be a method of choice for documenting hemodynamic insufficiency in the preoperative planning of infants suffering from early onset Moya-Moya's disease, a progressive obliterating angiopathy of major supratentorial vascular territories of the brain characterized by repeated transitory ischemic attacks (TIAs) and ischemic stroke.[47]

Also, PET/MRI may be used for independent simultaneous evaluation of new MRI perfusion techniques using PET as the 'golden' standard. There are initiatives to render improved ASL sequences more widely available. Furthermore, our method allows advanced combinations of standard and modern MRI techniques with molecular PET imaging, as have been shown in, e.g. pediatric neurooncology.[60,61]

No previous studies of ^{15}O-water PET rCBF in healthy newborn infants have been done. We obtained good quality images in four healthy newborns using a new PET/MRI method with an IDIF. We used improved diagnostic methods with a substantially lower radiation dose than the few existing previous studies performed in infants with pathology. The white/grey matter CBF ratio was close to that measured in the healthy human adult brain. The method may be useful as a 'golden' standard for evaluating new MR-based methods as well as for clinical research in specific disease states.

Funding

The author(s) disclosed receipt of the following financial support for the research, authorship, and/or publication of this article: This work was funded by The Ludvig and Sara Elsass Foundation. The hybrid PET/MRI system at Rigshospitalet was donated by the John and Birthe Meyer Foundation.

Acknowledgements

The authors thank Nuclear Medicine Technologists Marianne Federspiel, Karin Stahr, and Radiographer Jakup Madsen at the Department of Clinical Physiology, Nuclear Medicine and PET, and staff at the Department of Neonatology, University of Copenhagen for their valuable assistance before and during the scans. They also thank the Cyclotron Unit at the Department of Clinical Physiology, Nuclear Medicine and PET for reliable delivery of ^{15}O-water.

Declaration of conflicting interests

The author(s) declared no potential conflicts of interest with respect to the research, authorship, and/or publication of this article.

Authors' contributions

JBA contributed with design, recruitment of subjects, acquisition, analysis and interpretation of data, drafting and revising the manuscript and final approval of manuscript. UL contributed with design and analysis of data, revising and approving the manuscript, OO contributed with acquisition and analysis of data, revising and approving the manuscript, DB contributed in analysis and interpretation of data and approving the manuscript, CL contributed with design and analysis of data, revising and approving the manuscript, HL, contributed in analysis of data and revising and approving the manuscript, LH contributed with design and interpretation of data, revising and approving the manuscript, GG contributed with design, analysis and interpretation of data, revising and

approving the manuscript, IL contributed with design, analysis and interpretation of data, revising and approving the manuscript.

Supplementary material

Supplementary material for this paper can be found at the journal website: http://journals.sagepub.com/home/jcb

References

1. Banker BQ and Laarroche JC. Periventricular leukomalacia of infancy. A form of neonatal anoxic encephalopathy. *Arch Neurol* 1962; 7: 386–410.
2. Elitt CM and Rosenberg PA. The challenge of understanding cerebral white matter injury in the premature infant. *Neuroscience* 2014; 276: 216–238.
3. Borch K and Greisen G. Blood flow distribution in the normal human preterm brain. *Pediatr Res* 1998; 43: 28–33.
4. Borch K, Lou HC and Greisen G. Cerebral white matter blood flow and arterial blood pressure in preterm infants. *Acta Paediatr* 2010; 99: 1489–1492.
5. Kinney HC, Brody BA, Kloman AS, et al. Sequence of central nervous system myelination in human infancy. II. Patterns of myelination in autopsied infants. *J Neuropathol Exp Neurol* 1988; 47: 217–234.
6. Chugani HT, Phelps ME and Mazziotta JC. Positron emission tomography study of human brain functional development. *Ann Neurol* 1987; 22: 487–497.
7. Herscovitch P, Markham J and Raichle ME. Brain blood flow measured with intravenous H2(15)O. I. Theory and error analysis. *J Nucl Med* 1983; 24: 782–789.
8. Raichle ME, Martin WR, Herscovitch P, et al. Brain blood flow measured with intravenous H2(15)O. II. Implementation and validation. *J Nucl Med* 1983; 24: 790–798.
9. Altman DI, Powers WJ, Perlman JM, et al. Cerebral blood flow requirement for brain viability in newborn infants is lower than in adults. *Ann Neurol* 1988; 24: 218–226.
10. Altman DI and Volpe JJ. Positron emission tomography in newborn infants. *Clin Perinatol* 1991; 18: 549–562.
11. Volpe JJ, Herscovitch P, Perlman JM, et al. Positron emission tomography in the newborn: extensive impairment of regional cerebral blood flow with intraventricular hemorrhage and hemorrhagic intracerebral involvement. *Pediatrics* 1983; 72: 589–601.
12. Wintermark P. Injury and repair in perinatal brain injury: insights from non-invasive MR perfusion imaging. *Semin Perinatol* 2015; 39: 124–129.
13. De Vis JB, Petersen ET, de Vries LS, et al. Regional changes in brain perfusion during brain maturation measured non-invasively with Arterial Spin Labeling MRI in neonates. *Eur J Radiol* 2013; 82: 538–543.
14. De Vis JB, Hendrikse J, Petersen ET, et al. Arterial spin-labelling perfusion MRI and outcome in neonates with hypoxic-ischemic encephalopathy. *Eur Radiol* 2015; 25: 113–121.
15. Miranda MJ, Olofsson K and Sidaros K. Noninvasive measurements of regional cerebral perfusion in preterm and term neonates by magnetic resonance arterial spin labeling. *Pediatr Res* 2006; 60: 359–363.
16. Wintermark P, Hansen A, Gregas MC, et al. Brain perfusion in asphyxiated newborns treated with therapeutic hypothermia. *Am J Neuroradiol* 2011; 32: 2023–2029.
17. Wintermark P, Lechpammer M, Warfield SK, et al. Perfusion imaging of focal cortical dysplasia using arterial spin labeling: correlation with histopathological vascular density. *J Child Neurol* 2013; 28: 1474–1482.
18. Wintermark P, Hansen A, Warfield SK, et al. Near-infrared spectroscopy versus magnetic resonance imaging to study brain perfusion in newborns with hypoxic-ischemic encephalopathy treated with hypothermia. *Neuroimage* 2014; 85: 287–293.
19. Wintermark P, Lechpammer M, Kosaras B, et al. Brain perfusion is increased at term in the white matter of very preterm newborns and newborns with congenital heart disease: does this reflect activated angiogenesis? *Neuropediatrics* 2015; 46: 344–351.
20. Boudes E, Gilbert G, Leppert IR, et al. Measurement of brain perfusion in newborns: pulsed arterial spin labeling (PASL) versus pseudo-continuous arterial spin labeling (pCASL). *Neuroimage Clin* 2014; 6: 126–133.
21. Andersen JB, Henning WS, Lindberg U, et al. Positron emission tomography/magnetic resonance hybrid scanner imaging of cerebral blood flow using O-water positron emission tomography and arterial spin labeling magnetic resonance imaging in newborn piglets. *J Cereb Blood Flow Metab* 2015; 35: 1703–1710.
22. Zhang K, Herzog H, Mauler J, et al. Comparison of cerebral blood flow acquired by simultaneous [15O]water positron emission tomography and arterial spin labeling magnetic resonance imaging. *J Cereb Blood Flow Metab* 2014; 34: 1373–1380.
23. International Comission on Radiological Protection. The 2007 Recommendations of the International Commission on Radiological Protection. Report No.: 37, 2007.
24. European Commision. Radiation Protection 99. Guidance on mecical exposures in medical and biomedical research. https://ec europa eu/energy/sites/ener/files/documents/099_en pdf 1998 (accessed 19 December 2017).
25. International Comission on Radiological Protection. Radiological Protection in Biomedical Research. Report No.: 22, 1992.
26. Olesen OV, Wilm J, Van der Kouwe A, et al. An MRI compatible surface scanner. *ISMRM Sci Workshop* 2014; 1303.
27. Olesen OV, Sullivan JM, Mulnix T, et al. List-mode PET motion correction using markerless head tracking: proof-of-concept with scans of human subject. *IEEE Transac Med Imag* 2013; 32: 200–209.
28. Olesen OV, Paulsen RR, Hojgaard L, et al. Motion tracking for medical imaging: a nonvisible structured light tracking approach. *IEEE Transac Med Imag* 2012; 31: 79–87.
29. Ladefoged CN, Benoit D, Law I, et al. Region specific optimization of continuous linear attenuation coefficients based on UTE (RESOLUTE): application to PET/MR brain imaging. *Phys Med Biol* 2015; 60: 8047.

30. Meyer E. Simultaneous correction for tracer arrival delay and dispersion in CBF measurements by the H215O autoradiographic method and dynamic PET. *J Nucl Med* 1989; 30: 1069–1078.
31. Tanaka R, Spinale FG, Crawford FA, et al. Effect of chronic supraventricular tachycardia on left ventricular function and structure in newborn pigs. *J Am Coll Cardiol* 1992; 20: 1650–1660.
32. Slovis TL. Children, computed tomography radiation dose, and the As Low As Reasonably Achievable (ALARA) concept. *Pediatrics* 2003; 112: 971–972.
33. International Comission on Radiological Protection. Radiation Dose to Patients from Radiopharmaceuticals (Addendum to ICRP Publication 53). Report No.: 28, 1988.
34. Fung EK and Carson RE. Cerebral blood flow with [(15)O]water PET studies using an image-derived input function and MR-defined carotid centerlines. *Phys Med Biol* 2013; 58: 1903–1923.
35. Iida H, Miura S, Shoji Y, et al. Noninvasive quantitation of cerebral blood flow using oxygen-15-water and a dual-PET system. *J Nucl Med* 1998; 39: 1789–1798.
36. Mourik JE, van Velden FH, Lubberink M, et al. Image derived input functions for dynamic high resolution research tomograph PET brain studies. *Neuroimage* 2008; 43: 676–686.
37. Suhonen-Polvi H, Ruotsalainen U, Kinnala A, et al. FDG-PET in early infancy: simplified quantification methods to measure cerebral glucose utilization. *J Nucl Med* 1995; 36: 1249–1254.
38. Alvarez L, Aranega A, Saucedo R, et al. The quantitative anatomy of the normal human heart in fetal and perinatal life. *Int J Cardiol* 1987; 17: 57–72.
39. Tortora D, Mattei PA, Navarra R, et al. Prematurity and brain perfusion: arterial spin labeling MRI. *Neuroimage Clin* 2017; 15: 401–407.
40. van Gelderen P, de Zwart JA and Duyn JH. Pittfalls of MRI measurement of white matter perfusion based on arterial spin labeling. *Magn Reson Med* 2008; 59: 788–795.
41. Bokkers RP, Bremmer JP, van Berckel BN, et al. Arterial spin labeling perfusion MRI at multiple delay times: a correlative study with H(2)(15)O positron emission tomography in patients with symptomatic carotid artery occlusion. *J Cereb Blood Flow Metab* 2010; 30: 222–229.
42. Hendrikse J, van Osch MJ, Rutgers DR, et al. Internal carotid artery occlusion assessed at pulsed arterial spin-labeling perfusion MR imaging at multiple delay times. *Radiology* 2004; 233: 899–904.
43. Shi Y, Jin RB, Zhao JN, et al. Brain positron emission tomography in preterm and term newborn infants. *Early Hum Dev* 2009; 85: 429–432.
44. Shi Y, Zhao JN, Liu L, et al. Changes of positron emission tomography in newborn infants at different gestational ages, and neonatal hypoxic-ischemic encephalopathy. *Pediatr Neurol* 2012; 46: 116–123.
45. McArdle CB, Richardson CJ, Nicholas DA, et al. Developmental features of the neonatal brain: MR imaging. Part I. Gray-white matter differentiation and myelination. *Radiology* 1987; 162: 223–229.
46. Treyer V, Jobin M, Burger C, et al. Quantitative cerebral H2 15O perfusion PET without arterial blood sampling, a method based on washout rate. *Eur J Nucl Med Mol Imaging* 2003; 30: 572–580.
47. Kuhn FP, Warnock G, Schweingruber T, et al. Quantitative H 2 [15 O]-PET in pediatric moyamoya disease: evaluating perfusion before and after cerebral revascularization. *J Stroke Cerebrovasc Dis* 2015; 24: 965–971.
48. Watabe T, Shimosegawa E, Kato H, et al. CBF/CBV maps in normal volunteers studied with (15)O PET: a possible index of cerebral perfusion pressure. *Neurosci Bull* 2014; 30: 857–862.
49. Rostrup E, Knudsen GM, Law I, et al. The relationship between cerebral blood flow and volume in humans. *Neuroimage* 2005; 24: 1–11.
50. Ito H, Kanno I, Takahashi K, et al. Regional distribution of human cerebral vascular mean transit time measured by positron emission tomography. *Neuroimage* 2003; 19: 1163–1169.
51. Rostrup E, Law I, Blinkenberg M, et al. Regional differences in the CBF and BOLD responses to hypercapnia: a combined PET and fMRI study. *Neuroimage* 2000; 11: 87–97.
52. Lou HC, Lassen NA and Friis-Hansen B. Impaired autoregulation of cerebral blood flow in the distressed newborn infant. *J Pediatr* 1979; 94: 118–121.
53. Chugani HT and Phelps ME. Maturational changes in cerebral function in infants determined by 18FDG positron emission tomography. *Science* 1986; 231: 840–843.
54. Greisen G, Johansen K, Ellison PH, et al. Cerebral blood flow in the newborn infant: comparison of Doppler ultrasound and 133xenon clearance. *J Pediatr* 1984; 104: 411–418.
55. Mutsaerts HJ, Richard E, Heijtel DF, et al. Gray matter contamination in arterial spin labeling white matter perfusion measurements in patients with dementia. *Neuroimage Clin* 2014; 4: 139–144.
56. Deibler AR, Pollock JM, Kraft RA, et al. Arterial spin-labeling in routine clinical practice, part 2: hypoperfusion patterns. *Am J Neuroradiol* 2008; 29: 1235–1241.
57. Alsop DC, Detre JA, Golay X, et al. Recommended implementation of arterial spin-labeled perfusion MRI for clinical applications: a consensus of the ISMRM perfusion study group and the European consortium for ASL in dementia. *Magn Reson Med* 2014; 73: 102–116.
58. Kulak P, Maciorkowska E and Goscik E. Volumetric magnetic resonance imaging study of brain and cerebellum in children with cerebral palsy. *Biomed Res Int* 2016; 2016: 5961928.
59. Huppi PS, Warfield S, Kikinis R, et al. Quantitative magnetic resonance imaging of brain development in premature and mature newborns. *Ann Neurol* 1998; 43: 224–235.
60. Henriksen OM, Marner L and Law I. Clinical PET/MR imaging in dementia and neuro-oncology. *PET Clin* 2016; 11: 441–452.
61. Marner L, Henriksen OM, Lundemann M, et al. Clinical PET/MRI in neurooncology: opportunities and challenges from a single-institution perspective. *Clin Transl Imaging* 2017; 5: 135–149.